HHS Public Access

Author manuscript

Water Res. Author manuscript; available in PMC 2022 January 01.

Published in final edited form as:

Water Res. 2021 January 01; 188: 116534. doi:10.1016/j.watres.2020.116534.

Enhanced adsorption of per- and polyfluoroalkyl substances (PFAS) by edible, nutrient-amended montmorillonite clays

Meichen Wang[a], **Asuka A. Orr**[b], **Joseph M. Jakubowski**[b], **Kelsea E. Bird**[b], **Colleen M. Casey**[b], **Sara E. Hearon**[a], **Phanourios Tamamis**[b,c], **Timothy D. Phillips**[a,*]

[a]Department of Veterinary Integrative Biosciences, College of Veterinary Medicine and Biomedical Sciences, Texas A&M University, College Station, TX 77843, USA

[b]Artie McFerrin Department of Chemical Engineering, Texas A&M University, College Station, TX 77843, USA

[c]Department of Materials Science and Engineering, Texas A&M University, College Station, TX 77843, USA

Abstract

Humans and animals are frequently exposed to PFAS (per- and polyfluoroalkyl substances) through drinking water and food; however, no therapeutic sorbent strategies have been developed to mitigate this problem. Montmorillonites amended with the common nutrients, carnitine and choline, were characterized for their ability to bind 4 representative PFAS (PFOA, PFOS, GenX, and PFBS). Adsorption/desorption isothermal analysis showed that PFOA, PFOS (and a mixture of the two) fit the Langmuir model with high binding capacity, affinity and enthalpy at conditions simulating the stomach. A low percentage of desorption occurred at conditions simulating the intestine. The results suggested that hydrophobic and electrostatic interactions, and hydrogen bonding were responsible for sequestering PFAS into clay interlayers. Molecular dynamics (MD) simulations suggested the key mode of interaction of PFAS was through fluorinated carbon chains, and confirmed that PFOA and PFOS had enhanced binding to amended clays compared to GenX and PFBS. The safety and efficacy of amended montmorillonite clays were confirmed in *Hydra vulgaris,* where a mixture of amended sorbents delivered the highest protection against a PFAS mixture. These important results suggest that the inclusion of edible, nutrient-amended clays with optimal affinity, capacity, and enthalpy can be used to decrease the bioavailability of PFAS from contaminated drinking water and diets.

*Correspondence: tphillips@cvm.tamu.edu.

Declaration of interests

The authors declare that they have no known competing financial interests or personal relationships that could have appeared to influence the work reported in this paper.

Supporting Information

The detailed methods for MD simulations are supplied as Supporting Information. Figure S1 shows the schematic decomposition of carnitine and PFAS. Figure S2 shows the scanning electron microscope images of sorbent materials. Figure S3, S4, and S5 show the representative binding modes of PFOA, GenX, and PFBS, respectively.

GRAPHICAL ABSTRACT

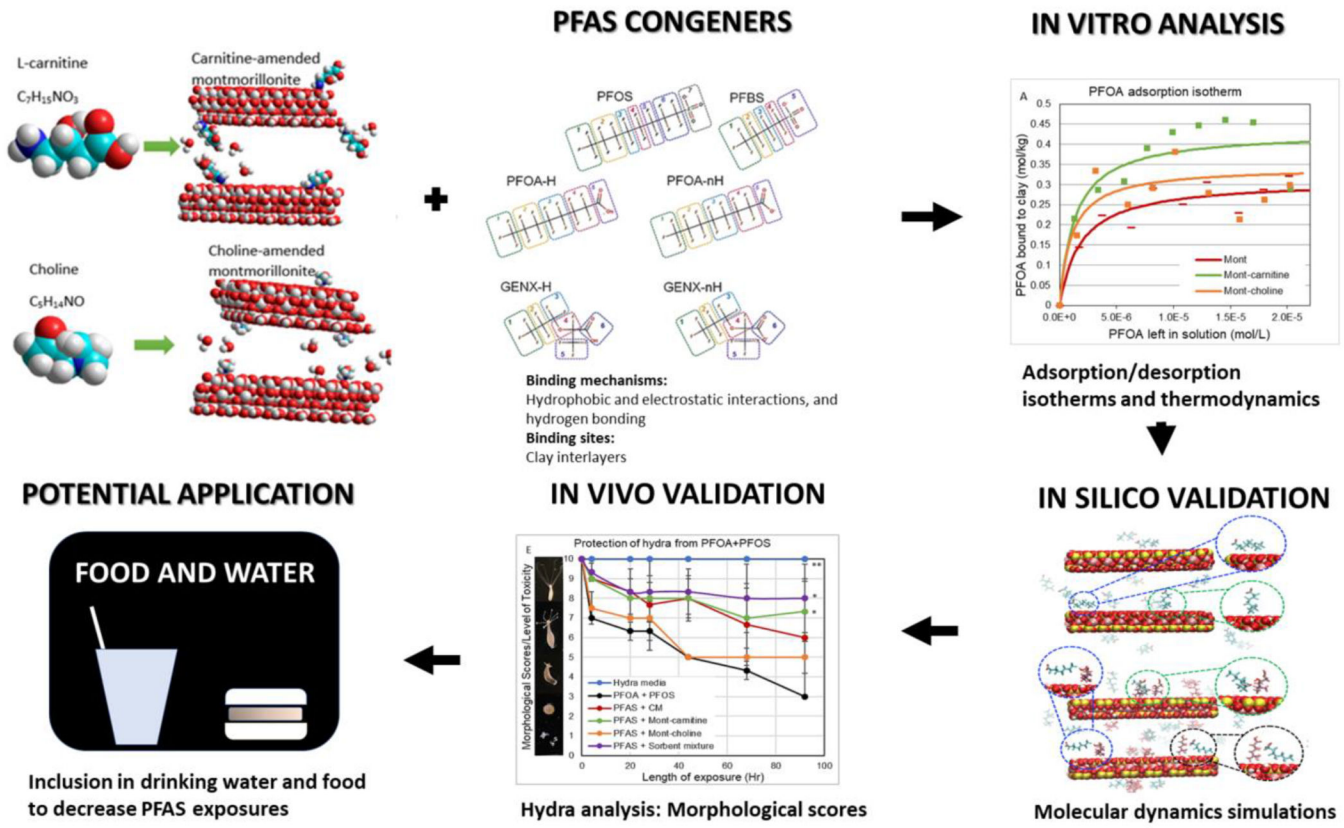

Keywords

PFAS; adsorption/desorption isotherms; hydra; montmorillonite clay; nutrient-amended clay; molecular dynamics simulations

1. Introduction

Per- and polyfluoroalkyl substances (PFAS) have been extensively used in numerous consumer and industrial products, such as firefighting foams, stain preventives, electronics, clothing, cookware, and lubricants, due to their high thermal stability and water, dust and oil repellency (EPA, 2017a). However, the high persistency, bioaccumulation, and widespread use of PFAS have resulted in their ubiquitous distribution in the environment (EPA, 2017a). The CDC's National Health and Nutrition Examination Survey (NHANES) reported that detectable PFAS concentrations were found at a frequency of 97% in 1682 blood samples from non-institutionalized American civilian residents (Lewis et al., 2015). Among PFAS, PFOA (perfluorooctanoate) and PFOS (perfluorooctanesulfonate) have been widely found in sediment, sludge, municipal wastewater, coastal water, and even tap water (EPA, 2016; 2017a). Because of their low pKa values, PFOS and PFOA predominantly exist as anions in environmentally relevant scenarios (ITRC, 2017). Furthermore, PFOA and PFOS have been shown to co-occur in a variety of drinking water sources (EPA, 2016; 2017a). To decrease

the use of the highly persistent and cumulative PFOA and PFOS, short-chain PFAS congeners, including GenX (hexafluoropropylene oxide) and PFBS (perfluorobutane sulfonic acid) were introduced as alternatives (ITRC, 2017). However, the hydrophobic chain and hydrophilic functional groups allow PFAS residues to be easily transported in an aquatic environment and adsorbed onto the surfaces of environmental solid matrices (Shih and Wang, 2013). This problem can be exacerbated during disasters, such as floods, chemical spills, and fires, where chemicals such as PFAS can be mobilized and redistributed in the environment, further threatening the safety of drinking water and food supplies (Wang and Phillips, 2019).

Many studies have reported that the adsorption and purification of wastewater containing PFAS can be economically feasible and effective (Zhang et al., 2019). Among conventional sorbents, powdered activated carbon (AC) has been shown to have the highest adsorption ability, and as early as 2005, the 3M company reported 99% removal of PFOS using AC (Fujii et al., 2007). However, a major route for human and animal exposure to PFAS is through the ingestion of PFAS-contaminated drinking water, fish, food packaged or processed with PFAS-containing materials, and crops grown in contaminated soil or water (ATSDR, 2019; Crone et al., 2019; EPA, 2017a; b). Once PFAS (especially long-chain PFAS) is consumed by animals and humans, it is absorbed, accumulated, and can be biomagnified through the food chain, causing adverse health effects such as cancer, immune system dysfunction, and liver damage (ATSDR, 2018). However, there are no reported strategies that can reduce unintended exposures through consumption of PFAS and PFAS mixtures in contaminated drinking water and foods.

It was reported that minerals played important roles in the PFAS sorption process. In groundwater systems, the fate and transport of PFAS have a strong dependence on interactions with surrounding mineral surfaces (Higgins and Luthy, 2006). Montmorillonite is a common form of hydrated aluminum oxide that usually exists as fine-grained constituents in soils and sediments. Importantly, calcium montmorillonite has been shown to be safe for the consumption of humans and animals based on multiple clinical trials and animal intervention studies (Phillips et al., 2019). To further enhance the lipophilicity of the clay surfaces, montmorillonite clay was amended with L-carnitine (mont-carnitine) or choline (mont-choline), which are natural nutrients that are commonly included in dietary supplements. Mont-carnitine and mont-choline have been previously shown to adsorb lipophilic environmental chemicals such as aflatoxin, benzo[a]pyrene, plasticizers, and pesticides (Cruz-Guzman et al., 2004; Orr et al., 2020; Wang et al., 2017; 2019). Thus, they were tested in this study for the adsorption of important PFAS chemicals and common mixtures. The mechanism of this strategy involves the ingestion of sorbent and the adsorption of PFAS by the sorbent in the stomach and intestines, resulting in reduced PFAS bioavailability.

The overall objective of this study was to investigate the binding of 4 common PFAS to the active surfaces of carnitine- and choline-amended montmorillonite clays versus the parent clay. We have characterized and optimized PFAS-sorbent interactions and binding parameters including *in vitro, in vivo* and *in silico* methods to: 1) determine equilibrium adsorption and desorption of PFAS from clay surfaces using isothermal analysis at

conditions that simulate the gastrointestinal tract, 2) identify active binding sites using heat-collapsed sorbents, 3) use molecular dynamics (MD) simulations to validate binding percentages and binding modes, 4) use thermodynamic studies to determine the heat of sorption (enthalpy), and 5) predict the safety and efficacy of sorbent interactions for individual PFAS and PFAS mixtures.

2. Materials and methods

2.1 Reagents and materials

High-performance liquid chromatography (HPLC)-grade acetonitrile and pH buffers (4.0, 7.0, and 10.0) were purchased from VWR (Atlanta, GA, USA). Analytical standards for PFAS were obtained from Sigma Aldrich (St. Louis, MO). Parent montmorillonite with a generic formula of $(Na,Ca)_{0.3}(Al,Mg)_2Si_4O_{10}(OH)_2 \cdot nH_2O$ was obtained from BASF (Lampertheim, Germany) with a total surface area of approximately 850 m^2/g, an external surface area of 70 m^2/g, cation exchange capacity equal to 97 cmol/kg, and a zeta potential of −31 mV (Kumar et al., 2020). Nutrient-amended montmorillonite clays were produced by intercalating L-carnitine or choline at 100% cation exchange capacity between interlayer surfaces under acidic conditions as previously described (Wang et al., 2017). MD simulations have shown that carnitine and choline are stably bound (with limited dissociation) to interlayer surfaces of montmorillonite clays (Orr et al., 2020). Mont-carnitine and mont-choline have been previously characterized for d_{001} interlayer spacing, composition of matter, and functional groups using x-ray diffraction (XRD) and fourier-transform infrared (FTIR) (Jaynes and Zartman, 2011; Velazquez and Deng, 2020). Collapsed clays were produced by heating at 200°C for 30 min and 800°C for 1 hr, resulting in the removal of structural water and dehydroxylation of the interlayers (Hedley et al., 2007). Thermogravimetric analysis (TGA) of montmorillonite clays has also suggested that exotherms indicating the formation of new phases occur at 1000°C and greater (Hedley et al., 2007). All sorbents were sieved at 325 mesh to achieve uniform particle size equal to, or less than 44 microns. The surface morphologies of all sorbents were investigated using a Tescan Vega3 scanning electron microscope (SEM) (Tescan Orsay Holding, a.s., Brno, Czech Republic) at 20 kV with a secondary electron detector at 5 kV accelerating voltage. Ultrapure deionized water (18.2 MΩ) was generated using an Elga™ automated filtration system (Woodridge, IL, USA).

2.2 Determination of pHpzc

The pH of point of zero charge (pH_{PZC}) was measured in this study since it has been previously reported to closely affect the binding affinity of PFOA and PFOS (Zhi and Liu, 2016). As previously described by Park et al. (2020), 100 mg of sorbents were added into 20 mL 0.1 M NaCl solutions with different initial pH values ranging from 2 to 11 adjusted with 0.5 N HCl or NaOH solutions. Before making the solution, distilled and deionized water was boiled to remove dissolved CO_2. Sealed vials were shaken for 48 hr at 200 rpm at room temperature. Subsequently, the final pH of the supernatant of the solution was measured when sorbents were completely settled. If the pH of the NaCl solution did not change after contact with sorbent, that pH was selected as pH_{PZC} of the sorbent.

2.3 Chemical analysis

PFAS was analyzed using a Waters Acquity ultraperformance liquid chromatography/tandem mass spectrometer (LC/MS-MS) equipped with triple quadrupole (Liang and Chang, 2019; Roberts et al., 2017). An Acquity BEH C18 column (2.1 × 50 mm, 1.7 μm) was used for separation and kept at 40°C in the column oven. A gradient elution using 20 mM ammonium acetate (eluent A) and acetonitrile (eluent B) was carried out at a flow rate of 0.6 mL/min. The gradient program for elution was 10% eluent B (initial), 10%-55% (0 to 0.1 min), 55%-99% (0.1 to 4.5 min), 99% (4.5 to 5 min), and 99%-10% (5 to 6.5 min). The injection volume was 10 μL for each analysis. The mass spectrometer was used with an electrospray ionization interface (ESI) and operated in a negative ion mode. The spray voltage was maintained at 4.5 kV. The source temperature was kept at 450°C. The monitored precursor and product ions (m/z) for PFOA, PFOS, GenX, and PFBS were 413 to 369, 499 to 80, 285 to 168.9, and 298.9 to 80, respectively. The cone voltage (kV) for PFOA, PFOS, GenX, and PFBS was 25, 40, 20, and 35, respectively. The mass spectrometer was operated under multiple reaction monitoring (MRM) mode. Nitrogen gas was used as the collision and curtain gas, and argon gas was used as the nebulizer and heater gas. Empower analyst software was used to control the LC/MS-MS system and acquire the data.

2.4 Adsorption isotherms

PFAS solutions, including PFOA, PFOS, GenX, and PFBS, at a concentration of 5 ppm (μg/mL) were individually prepared from pure crystals in pH 2 distilled water, which is the average stomach pH. The concentrations were set based on previous literature (Zhi and Liu, 2016), screening results, and the optimal ratio of sorbent/PFAS to achieve equilibrium (saturation) on isotherm plots. Each sorbent at 0.0005% was then added to a concentration gradient from 5% to 100% of 5 mL of PFAS solution. Controls included 5 mL of blank solution (pH 2 water), PFAS solution, and sorbent suspension. All samples were vibrated at 1000 rpm and 37°C or 24°C using an IKA® electric shaker (VIBRAX VXR basic, Werke, Germany) for 2 hr, as 2 hr is the average digestion time in a human stomach. The sorbent/PFAS complex was then separated from solution by centrifugation at 2000 g for 20 min and the supernatant was analyzed by LC/MS-MS.

2.5 Desorption isotherms

The desorption of PFAS from the surface of sorbents was tested in a simulated intestine model. At the end of adsorption experiments, PFAS-loaded sorbents were separated from the aqueous solutions and rinsed once with pH 7 water to washout unbound PFAS and traces of acid. The tubes were then filled with 5 mL of pH 7 water solution and shaken at 200 rpm and 37°C for 48 hr on a rocking platform (VMR, PA, USA). The 48 hr equilibration time was chosen based on the maximum duration of digestion in human intestines. Then the suspensions were centrifuged at 2000 g for 20 min, and an aliquot of supernatant was extracted for analysis. Desorbed PFAS concentrations were detected at the end of the desorption experiment and the amount of PFAS that remained bound on sorbents was determined as the difference between the initial adsorbed and the desorbed amount. For both adsorption and desorption, the dry weight of sorbents, before and after, the experiments were determined for selected concentrations, and no significant change was observed. The

potential variability in the amount of PFAS adsorbed and desorbed to clay surfaces based on isothermal data calculations was less than 4% relative standard deviation.

2.6 Data calculations and curve fitting

PFAS detected by LC/MS-MS was calculated to determine the free PFAS concentrations in solution. In the adsorption study, the quantity of bound PFAS was calculated by the concentration difference between control and test groups and expressed as mol/kg on the isotherm plots. The amount of PFAS that remained bound in the desorption study was derived from the difference between the initial amount bound in the adsorption and the dissociation in the solution. Table-Curve 2D was used to plot these data and derive values for the variable parameters. The adsorption and desorption isotherms were plotted by well-established Langmuir or Freundlich models based on the equation that fit the data with highest correlation coefficients and randomness of the residuals from triplicate analyses (Grant and Phillips, 1998). The Langmuir isotherm describes monolayer adsorption onto a surface with a finite number of identical sites and uniform energies of adsorption. The Langmuir equation was entered as user-defined functions:

$$\text{Langmuir model} \qquad q = Q_{\max}\left(\frac{K_d C_w}{1 + K_d C_w}\right) \tag{1}$$

q = the amount of PFAS adsorbed (mol/kg), Q_{max} = maximum binding capacity (mol/kg), K_d = Langmuir distribution constant, C_w = equilibrium concentration of PFAS (mol/L).

The Freundlich isotherm is used to describe the adsorption characteristics for a heterogeneous surface. The Freundlich model is represented by the following equation:

$$\text{Freundlich model} \qquad q = K_f C_w^{1/n} \tag{2}$$

K_f = Freundlich distribution constant, 1/n = degree of heterogenicity.

The percentage of desorption was calculated by the following equation:

$$\%\ \text{Desorption} = 100x\left(1 - \frac{q_{\max}}{Q_{\max}}\right) \tag{3}$$

Q_{max} = maximum capacity in the adsorption study (mol/kg), q_{max} = remaining capacity in the desorption study (mol/kg).

2.7 MD simulations and structural analysis

The binding of PFAS (PFOA, PFOS, GenX, and PFBS), independently, with parent and carnitine-amended montmorillonite clays was investigated through quintet 50 ns MD simulations and subsequent structural analysis using in-house Fortran programs, analogous to our previous studies (Wang et al., 2019a). The deprotonated states of PFOS and PFBS were investigated since their pKa values can be as low as −3, which is significantly below the pH in the MD simulations (pH 2). While the deprotonated PFOA (PFOA-nH) is the main form in the environment, it is important to investigate both the deprotonated (PFOA-nH) and

protonated (PFOA-H) congeners of PFOA, since previous studies reported a wide range of possible pKa values (−0.5-3.8) (Burns et al., 2008; Steinle-Darling et al., 2008; Vierke et al., 2013). Additionally, due to the pKa values of GenX (2.8-3.8), both protonated (GenX-H) and deprotonated (GenX-nH) forms were investigated. The ratio of different protonation states between PFOA-H and PFOA-nH or GenX-H and GenX-nH was not considered, which was beyond the scope of our investigation. Thus, a total of 12 simulation systems were computationally investigated, corresponding to each of the 6 PFAS forms in the presence of the parent clay and mont-carnitine, independently. In the structural analysis, the propensity of PFAS binding to clays was evaluated through: 1) binding percentage calculations, and 2) prominent binding modes determined based on which chemical groups of PFAS, as shown in Figure S1, interact with the clays. The MD simulations and subsequent structural analysis are described in detail in the Supporting Information.

2.8 Hydra assay

Hydra vulgaris were obtained from Environment Canada (Montreal, Qc) and maintained at 18°C. Using a hydra classification method, the morphology of hydra was rated over time as an indicator of solution toxicity. The morphological scoring of hydra was objective and repeatable (Dash et al., 2012; Hearon et al., 2020). The hydra response was scored after exposure to PFAS, with and without, sorbent inclusion. The assay included closely monitoring mature and non-budding hydra at 0, 4, 20, 28, 44, 68, and 92 hr, without changing solutions during testing. Hydra medium was included as a control. PFAS dose-response groups consisted of PFOA, PFOS, and a mixture of PFOA and PFOS at a gradient of concentrations to determine the minimum effective doses that resulted in 100% mortality of hydra in 92 hr. Individual sorbents and a sorbent mixture of equal amounts of amended clays were added to the PFAS solutions at 0.02% inclusion rate. All solutions were mixed at 1000 rpm for 2 hr and centrifuged at 2000 g for 20 min prior to exposure of hydra in Pyrex dishes. Three hydra colonies in each group were exposed to 4 mL of test medium at 18°C. The average score for each group was used to determine the toxicity rating at each time point.

A two-way t-test was used to determine statistical significance. Each experiment was independently conducted in triplicate to derive means and standard deviations for the toxicity scores from the hydra assay. These were then used to calculate the t-value using a Tukey test and p-value. Results were considered significant at $p \leq 0.05$.

3. Results and discussion

Clays have been used as ancient medicine for diarrhea, cholera, bacterial infections, and mitigation of poisonings. For centuries, eating clay has been a global practice that exists among humans as well as numerous animal species. In previous intervention studies and clinical trials in the US and Africa, calcium montmorillonite clay was shown to be safe for human and animal consumption. However, the clay had a preference for binding aflatoxins and certain hydrophilic chemicals (Phillips et al, 2019; Wang et al., 2019). To enhance its ability to bind diverse environmental chemicals, we amended the interlayer with L-carnitine

and choline, to increase interlayer spacing (Figure S2) and hydrophobicity of the clay surfaces.

A 7-point standard curve for each PFAS was constructed using concentrations ranging from the limit of detection (LOD) to 10 ppm. LOD was determined to be 10 ppb with a signal-to-noise ratio equal to 3. The calibration solutions were prepared daily and verified before running test samples. The linearity (r^2) in all cases was $1 > r^2 > 0.99$.

3.1 Adsorption analyses

Adsorption isotherms were conducted using a simulated stomach model at pH 2 and 37°C for 2 hr to simulate the average duration of the digestion process in the stomach. Isothermal data reflecting the sorption of PFOA and PFOS onto clay surfaces were plotted as a Langmuir model based on their r^2 values. As shown in Figure 1A and 1B, the adsorption plots of PFOA and PFOS binding onto parent montmorillonites exhibited good fit to a Langmuir model based on correlation coefficients and a curved shape, suggesting the presence of monolayer binding and saturable active sites. The binding of PFOA and PFOS onto parent montmorillonite clay showed high capacities equal to 0.31 and 0.58 mol/kg, and high affinities equal to 5.37E5 and 1.81E5, respectively. Within MD simulations, the binding percentages of deprotonated PFOA-nH and PFOS onto parent clay were 20±3% and 18±2%, respectively (Figure 2). This agrees with the higher affinity of PFOA versus PFOS observed in the isothermal studies. The higher binding propensity of PFOA-H could be facilitated by hydrogen bonding to the clay interlayer (Figure S3).

Furthermore, our isothermal results indicated that amendments of montmorillonite clay with carnitine and choline enhanced the binding capacity for PFOA to 0.43 and 0.34 mol/kg, compared to parent clay. Similarly, PFOS binding capacity was increased for mont-carnitine (Q_{max} = 0.73 mol/kg) and mont-choline (Q_{max} = 0.75 mol/kg), compared to parent montmorillonite (Figure 1A and 1B). The improved binding of mont-carnitine for PFOA (both PFOA-nH and PFOA-H) and PFOS was also observed within MD simulations where mont-carnitine showed significantly higher binding percentages than the parent clay (Figure 2). This improvement of mont-carnitine was more pronounced for protonated PFOA-H than deprotonated PFOA-nH, presumably due to the neutral charge on PFOA-H. Both PFOA and PFOS were shown to bind to carnitine directly, or bind to clay interlayer and carnitine simultaneously (Figure 2). This enhancement in PFOA and PFOS binding from the addition of L-carnitine and choline (at acidic pH) may involve the exchange of inorganic cations and an increase of the hydrophobicity at interlayer surfaces, resulting in a reduction of polar charge and more hydrophobic surfaces that facilitate the binding of PFAS.

To further investigate the hydrophobic interaction, short-chain PFAS including GenX and PFBS were tested by isothermal analysis. Contrary to the isothermal plots of PFOA and PFOS, the binding of GenX and PFBS was best described by a Freundlich (partitioning) model as suggested by the r^2 and the plots in Figure 1C and 1D. This indicated heterogeneous binding sites, the lack of a saturable (specific) site on the clay surfaces, and a partitioning interaction.

According to the MD simulations, GenX (both GenX-H and GenX-nH) and PFBS bind both in the interlayer and at basal surface sites on the clay, supporting the heterogenous binding shown in the Freundlich isotherms. While the protonated GenX (GenX-H) binds to the parent clay with a similar propensity as PFOA and PFOS, the deprotonated GenX (GenX-nH) and PFBS bind with less propensity (Figure S4). Although mont-carnitine slightly enhanced the binding of GenX and PFBS, PFOA and PFOS showed higher binding to both parent and carnitine-amended clays, compared to GenX and PFBS (Figure 2). This trend complies with experimental results showing that PFOA and PFOS bind to the clay through homogenous adsorption with saturable capacity, while GenX and PFBS bind to the clay through heterogeneous surface adsorption and partitioning activity. The decrease of homogenous binding sites and the lack of a Q_{max} for GenX and PFBS could be due to less hydrophobicity, compared to long-chain PFAS. The prominent binding modes of GenX and PFBS to parent and mont-carnitine clays are presented in Figure S4 and S5, respectively.

The extensive use and widespread distribution of PFAS are long-standing, especially for the legacy PFOA and PFOS that are highly persistent. The scientific literature has shown the co-occurrence of PFOA and PFOS in drinking water at the same time and location (EPA, 2016; 2017a), therefore, isothermal analysis was conducted with co-exposure to equal concentrations of PFOA and PFOS. Results in Figure 3 showed that adsorption of the mixture onto amended montmorillonites maintained a good fit to the Langmuir model with slightly lower Q_{max} values, compared to exposure to individual PFAS. Despite the slight decrease, binding onto mont-carnitine and mont-choline remained high with Q_{max} equal to 0.42 and 0.31 mol/kg for PFOA and 0.71 and 0.69 mol/kg for PFOS, respectively. Similar to isotherms with individual toxicants in Figure 1, adsorption of PFOS showed higher binding capacity than PFOA, which is consistent with the literature (Yu and Hu, 2011; Zhao et al., 2014; Zhang et al., 2019). This was possibly attributed to the higher water solubility of PFOA and its higher attraction to water molecules versus PFOS (Cooney, 1998).

As part of this study, it was important to gain insight into the thermodynamics of toxicant/surface interactions. The enthalpy (heat) of sorption (ΔH) can be calculated from K_d values of isotherms run at different temperatures, i.e., 37°C and 24°C (Figure 4). It is directly relevant to the tightness of toxicant/clay interactions and can help with the derivation of mechanistic information. In particular, the sorption of compounds to a surface can be categorized as either physisorption or chemisorption based on ΔH. Calculated enthalpies (ΔH) for PFOA onto montmorillonite, mont-carnitine, and mont-choline were equal to −57, −96.6, and −77.7 kJ/mol, respectively. Enthalpies for PFOS were −43.1, −50.6, and −41.3 kJ/mol for montmorillonite, mont-carnitine, and mont-choline, respectively. These high enthalpy absolute values (> 20 kJ/mol) indicated that PFOA and PFOS were tightly bound to clay surfaces, which is consistent with the Langmuir model for the isothermal interaction.

Adsorption parameters for PFAS/clay interactions are shown in Table 1. All of the correlation coefficient values for the Langmuir and Freundlich models were greater than 0.8. Also, the standard deviations were lower than 4%, and all points had small deviations from the plots supporting the validity of these models for describing the PFAS adsorption process. Blank controls for each PFAS, without sorbent, were performed and confirmed that PFAS precipitation did not occur and was not associated with PFAS sorption.

3.2 Major binding sites and modes

Clays were heat-treated to determine the importance of interlayer surfaces in the binding of PFOA and PFOS. Heating clays at 200°C and 800°C have been shown to significantly collapse the interlayer surfaces, thus reducing the amount of total binding sites available. The isothermal plot in Figure 5 shows that the adsorption regressed to a Freundlich trend for heat-collapsed clays without a Q_{max} value ($r^2 > 0.92$). The values of distribution constants were significantly decreased from 10^5 in intact clays to less than 10^2 ($p \leq 0.01$). This result indicates that the interlayer was a major binding site that contributed to saturable and homogenous binding, possibly explaining higher binding of PFOA and PFOS onto amended clays due to their higher interlayer spacing (Figure S2) (Jaynes and Zartman, 2011). The binding on the remaining basal surfaces and edge sites was minor and showed a partitioning activity. Also, previous XRD analysis indicated the adsorption of PFOS in the interlayer of a sodium montmorillonite clay with increased d_{001} spacing (Zhou et al., 2010).

Within the MD simulations, structural analysis of the binding instances of the deprotonated PFOA-nH and PFOS showed that both molecules are predominantly bound to the parent clay interlayer through hydrophobic interactions with the fluorinated carbon chains. Specifically, in 79% of the binding instances, PFOA-nH interacted with the clay through the terminal end of its fluorinated carbon chains (Figure 6A, encircled in green), while 19% of PFOA-nH interacted through the entire fluorinated carbon chain (Figure 6A, encircled in blue). Similar to PFOA-nH, in 52% of the binding instances, PFOS interacted with the clay through the terminal end of its fluorinated carbon chains (Figure 6B, encircled in green), while 20% of PFOS interacted at basal sites of clay through the entire fluorinated carbon chains (Figure 6B, encircled in blue). It is worth noting that the number of basal binding instances of PFOS may be overestimated by the modeled system. This result shows that PFOA-nH and PFOS mainly bind to the clay surfaces through hydrophobic tails, suggesting that hydrophobic interaction is the major binding mechanism for montmorillonite clay, which agrees with the earlier conclusion. The higher binding of toxicants at the terminal end of the fluorinated carbon chain could be related to electrostatic interaction between partially negative fluorines and positive clay surfaces at pH 2.

Besides hydrophobic and electrostatic interactions, hydrogen bonding could also contribute to the higher binding onto amended clays. According to MD simulations, in 42% of assisted binding instances, protonated and deprotonated PFOA bind to mont-carnitine by hydrogen bonds between its carboxyl group and the carboxyl or hydroxyl group on carnitine. In this binding mode, PFOA was shown to simultaneously bind to clay interlayers through the terminal end of its fluorinated carbon chain (Figure 6C and S3C). PFOA also participated in assisted-binding to mont-carnitine through either the terminal end of its fluorinated carbon chain (Figure 6C and S3D, 29% of assisted-binding instances) or the mid-portion of its fluorinated carbon chain (Figure 6C and S3E, 27% of assisted-binding instances). Similarly, PFOS predominantly participated in assisted-binding to mont-carnitine by forming hydrogen bonds between its sulfonate group (45% of assisted-binding instances), fluorinated carbon chain, or the terminal end of its fluorinated carbon chain (22% of assisted-binding instances) and the hydroxyl group of amending carnitine (Figure 6D).

3.3 Desorption analysis

Besides the high capacity and high affinity for binding in stomach conditions, stability and tightness of the adsorption complex are important in the evaluation of the potential for PFAS dissociation in conditions simulating the intestine. Therefore, desorption studies were run using PFAS-loaded sorbents following the adsorption study, and these were suspended in pH 7 water and incubated at 37°C for 48 hr to simulate the intestine. The amount of PFAS remaining bound after dissociation (q_{max}) was calculated from the difference between the maximum adsorption value Q_{max} and the dissociated concentration in the solution. The q_{max} values were lower compared to Q_{max} values of their adsorption isotherms. The point of zero charge (PZC) of mont-carnitine and mont-choline were determined to be pH 9.3 and 10, respectively. Therefore, the overall positive charge on the surfaces of these amended clays may result from the solution at a pH lower than pH_{PZC}, and oversaturation during cation exchange. The protonated surfaces on amended clays attracted PFAS that is negatively charged. Therefore, the increase of solution pH from 2 to 7 can decrease the positive sites on the clay surfaces, resulting in the desorption of PFOA and PFOS with reduced q_{max} and K_d.

From the results in Figure 7, adsorption isotherms after desorption of PFOA and PFOS from amended clays maintained a Langmuir shape as suggested by $r^2 \geq 0.9$ (Table 2), indicating the persistence of saturable binding sites during the dissociation. The desorption percentages are less than 12% for both PFOA and PFOS. All these suggest that only a small amount of bound PFAS was dissociated from the binding complex in the intestine model. These results further indicate that PFOA and PFOS binding to amended clays involve tight interactions, and the complex is expected to be stable and not easily desorbed in the intestine. The consistently higher binding affinity in mont-choline compared to mont-carnitine in all adsorption isotherms possibly resulted from the slightly higher pH_{PZC} of mont-choline (10), since pH_{PZC} was reported to closely correlate to PFAS binding affinity (Zhi and Liu, 2016).

3.4 Hydra assay

Hydra vulgaris is very sensitive to environmental toxins and has been widely used as an indicator of toxicity. It has accurately predicted the safety and efficacy of toxin-binding sorbents from diverse *in vivo* studies (Afriyie-Gyawu et al., 2005; Marroquin-Cardona et al., 2009; Wang et al., 2019b; Wang and Phillips, 2020). It has also been utilized along with an *in vitro* gastrointestinal model (Lemke et al., 2001; Wang et al., 2020) and *in silico* MD simulations (Orr et al., 2020) for obtaining fundamental insight, and for screening and validation purposes. The toxicities of individual PFOA and PFOS and a mixture of PFOA and PFOS were determined by the *hydra vulgaris* assay using minimum effective doses (MEDs) equal to 100 ppm PFOA, 100 ppm PFOS, and 90 ppm of the binary mixture (Figure 8A, C, E). The inclusion of only 0.02% w/v mont-carnitine and mont-choline with PFOA show significant protection of hydra (93±4.71% and 100%), versus 89% with parent montmorillonite, $p \leq 0.01$ (Figure 8B). Additionally, mont-carnitine and mont-choline reduced 60±8.16% and 63±4.71% PFOS toxicity ($p \leq 0.01$), compared to 60±8.16% from the parent clay (Figure 8D). Furthermore, to test sorption efficacy for PFOA and PFOS mixtures, individual sorbents and a mixture of 50% mont-carnitine and 50% mont-choline were administered at 0.02%. Results in Figure 9E show that the mixture showed significant protection at 71±17.3% against the PFOA and PFOS mixture ($p \leq 0.05$). This protection

percentage was higher than individual mont (43±30%), mont-carnitine (62±15.3%), and mont-choline (29±8.2%), indicating a mixture of optimal sorbents can effectively reduce the toxicity of PFAS mixtures. It is possible that higher doses of sorbents will contribute to even better protection against toxicity, based on previous dosimetry studies (Hearon et al., 2021; Maki et al., 2017; Phillips et al., 2008; Wang et al., 2019c). Based on previous correlations between isothermal capacity, dosimetry and human intervention studies, an estimation of 0.25% sorbent inclusion in drinking water and the diet could be effective in mitigating PFAS exposures.

Mitigation strategies for PFAS have focused mainly on the purification of contaminated wastewater, not drinking water and food. Current recommendations to reduce consumption of PFAS trough drinking water and food include: 1) minimizing exposure to food packaging, 2) testing local tap water for contamination, and 3) using bottled water (Consumer Reports, 2019; Department of Health, 2020). Based on the results from the current study, the dietary inclusion of edible, amended clays with high affinity, capacity, enthalpy, and tightness for PFAS and the ability to reduce exposures and related toxicity from contaminated food and water would be an alternative strategy.

Since PFAS have unique physicochemical properties that vary with chain length, functional group, and degree of fluorination, ongoing studies are necessary for the development of a combination of broad-acting sorbents to reduce exposures to mixtures of PFAS.

4. Conclusions

- In this study, we characterized PFAS binding ability of montmorillonite clays that were amended with the natural nutrients, carnitine and choline, by isothermal analysis, MD simulations, and the hydra assay.
- Using simulated conditions found in the stomach and intestine, amended montmorillonite clays showed high binding efficacy for PFOA, PFOS and a mixture of the two based on high binding percentage, capacity, affinity, correlation coefficient, enthalpy, and tightness.
- Hydrophobic and electrostatic interactions were responsible for sequestering long-chain PFAS into clay interlayers, while hydrogen bonding interactions also contributed to the binding of PFAS.
- *H. vulgaris* confirmed the safety of these sorbents and the ability of the interaction to decrease the toxicity of PFAS mixtures.
- Our results show that these edible sorbents have a notable potential for the detoxification of important long-chain PFAS and their mixtures from drinking water and the diet. Further studies are warranted to investigate the effectiveness of these clays when added to flavored drinking water, snacks, condiments, and various foods.

Supplementary Material

Refer to Web version on PubMed Central for supplementary material.

Acknowledgments

This work was supported by the Superfund Hazardous Substance Research and Training Program (National Institutes of Health) [P42 ES027704]; and the United States Department of Agriculture [Hatch 6215]. Analytical standards of PFAS were gifts from Dr. Tony Knap (Texas A&M University Geochemical & Environmental Research Group) and Dr. Kung-Hui Chu (Texas A&M University).

References

Afriyie-Gyawu E; Wiles MC; Huebner HJ; Richardson MB; Fickey C; Phillips TD Prevention of zearalenone-induced hyperestrogenism in prepubertal mice. Toxicol. Environ. Health A. 2005, 68(5), 353–368.

Agency for Toxic Substances and Disease Registry. How can I be exposed to PFAS. 2019 https://www.atsdr.cdc.gov/pfas/pfas-exposure.html

Agency for Toxic Substances and Disease Registry. Toxicological Profile for Perfluoroalkyls (Draft for Public Comment. Department of Health and Human Services, Public Health Service 2018 https://www.atsdr.cdc.gov/toxprofiles/tp.asp?id=1117&tid=237

Burns DC; Ellis DA; Li H; McMurdo CJ; Webster E Experimental pKa determination for perfluorooctanoic acid (PFOA) and the potential impact of pKa concentration dependence on laboratory-measured partitioning phenomena and environmental modeling. Environ. Sci. Technol 2008, 42(24), 9283–9288. [PubMed: 19174905]

Consumer Reports. To Reduce PFAS Levels in Food, Cook at Home. https://www.consumerreports.org/food-safety/to-reduce-pfas-levels-in-food-cook-at-home/

Cooney DO (1998). Adsorption design for wastewater treatment, Lewis, New Jersey.

Crone BC; Speth TF; Wahman DG; Smith SJ; Abulikemu G; Kleiner EJ; Pressman JG Occurrence of per- and polyfluoroalkyl substances (PFAS) in source water and their treatment in drinking water. Environ. Sci. Technol 2019, 49(24), 2359–2396.

Cruz-Guzman M; Celis R; Hermosin MC; Cornejo J Adsorption of the Herbicide Simazine by Montmorillonite Modified with Natural Organic Cations. Environ. Sci. Technol 2004, 38(1), 180–186. [PubMed: 14740734]

Dash B; Phillips TD Molecular characterization of a catalase from hydra vulgaris. Gene, 2012, 501(2), 144–152. [PubMed: 22521743]

Fujii S; Tanaka S; Lien NPH; Qiu Y; Polprasert C New POPs in the water environment: distribution, bioaccumulation and treatment of perfluorinated compounds—a review paper. J. Water Supply Res. Technol 2007, 56, 313–326.

Grant PG; Phillips TD Isothermal adsorption of aflatoxin B1 on HSCAS clay. J. Agric. Food Chem 1998, 46(2), 599–605 [PubMed: 10554284]

Hearon SE; Wang M; Phillips TD Strong adsorption of dieldrin by parent and processed montmorillonite clays. Environ. Toxi. Chem 2020, 39(3), 517–525.

Hearon SE; Wang M; McDonald TJ; Phillips TD Decreased bioavailability of aminomethylphosphonic acid (AMPA) in genetically modified corn with activated carbon or calcium montmorillonite clay inclusion in soil. J. Environ. Sci 2021, 100, 131–143.

Hedley CB; Yuan G; Theng BKG Thermal analysis of montmorillonites modified with quaternaryphosphonium and ammonium surfactants. Appl. Clay Sci 2007, 35, 180–188.

Higgins CP.; Luthy RG. Sorption of perfluorinated surfactants on sediments. Environ. Sci. Technol 2006, 40, 7251–7256. [PubMed: 17180974]

Interstate Technology & Regulatory Council. Naming conventions and physical and chemical properties of per- and polyfluoroalkyl substances (PFAS). 2017 https://pfas-1.itrcweb.org/fact_sheets_page/PFAS_Fact_Sheet_Naming_Conventions_April2020.pdf

Jaynes WF; Zartman RE Aflatoxin toxicity reduction in feed by enhanced binding to surface-modified clay additives. Toxins. 2011, 3(6), 551–565. [PubMed: 22069725]

Kumar A; Hodnett BK; Hudson S; Davern P Modification of the zeta potential of montmorillonite to achieve high active pharmaceutical ingredient nanoparticle loading and stabilization with optimum dissolution properties. Colloids Surf. B. 2020, 193, 111–120.

Lemke SL; Ottinger SE; Mayura K; Ake CL; Pimpukdee K; Wang N; Phillips TD Development of a multi-tiered apprach to the in vitro prescreening of clay-based enterosorbents. Animal Feed Sci. Technol 2001, 93, 17–29.

Lewis RC; Johns LE; Meeker JD Serum Biomarkers of Exposure to Perfluoroalkyl Substances in Relation to Serum Testosterone and Measures of Thyroid Function among Adults and Adolescents from NHANES 2011–2012. Int. J. Environ. Res. Public Health. 2015 12(6), 6098–6114. [PubMed: 26035660]

Liang S; Chang M Integrating the Analysis of Ultrashort-Chain PFAS. 2019 https://www.restek.com/pdfs/EVAN3073-UNV.pdf

Maki CR; Haney S; Wang M; Ward SH; Rude BJ; Bailey RH; Harvey RB; Phillips TD Calcium montmorillonite clay for the reduction of aflatoxin residues in milk and dairy products. JDVS. 2017, 2(3), 1–8.

Marroquin-Cardona A; Deng Y; Taylor JF; Hallmark CT; Johnson NM; Phillips TD Characterization of mycotoxin binding agents used for animal feeds in México. Food. Addit. Contam 2009, 26(5), 733–743.

Orr AA; He S; Wang M; Goodall A; Hearon SE; Phillips TD; Tamamis P Insights into the interactions of bisphenol and phthalate compounds with unamended and carnitine-amended montmorillonite clays. Comput. Chem. Eng 2020, 143, 107063. [PubMed: 33122868]

Park M; Wu S; Lopez IJ; Chang JY; karanfil T; Snyder SA Adsorption of perfluoroalkyl substances (PFAS) in groundwater by granular activated carbons: Roles of hydrophobicity of PFAS and carbon characteristics. Water Res. 2020, 170, 115364. [PubMed: 31812815]

Phillips TD; Afriyie-Gyawu E; Williams J; Huebner H; Ankrah NA; Ofori-Adjei D; Jolly P; Johnson N; Taylor J; Marroquin-Cardona A; Xu L; Tang L; Wang JS Reducing human exposure to aflatoxin through the use of clay: A review. Food Addit. and Contam. Part A. 2008, 25(2), 134–145.

Phillips TD; Wang M; Elmore SE; Hearon S; Wang JS NovaSil clay for the protection of humans and animals from aflatoxins and other contaminants. Clays Clay. Miner 2019, 67(1), 99–110. [PubMed: 32943795]

Roberts S; Hyland KC; Butt C; Krepich S; Redman E; Borton C Quantitation of PFASs in Water Samples using LC-MS/MS Large-Volume Direct Injection and Solid Phase Extraction. Food and Environmental, 2017 https://sciex.com/Documents/tech%20notes/PFAS-water-samples.pdf

Shih K; Wang F Adsorption behavior of perfluorochemicals (PFCs) on boehmite: influence of solution chemistry. Procedia Environ. Sci 2013, 18, 106–113.

State of Rhode Island, Department of Health. PFAS Contamination of Water. https://health.ri.gov/water/about/pfas/

Steinle-Darling E; Reinhard M Nanofiltration for trace organic contaminant removal: structure, solution, and membrane fouling effects on the rejection of perfluorochemicals. Environ. Sci. Technol 2008, 42(14), 5292–5297. [PubMed: 18754383]

United State Environmental Protection Agency. Technical Fact Sheet – Perfluorooctane Sulfonate (PFOS) and Perfluorooctanoic Acid (PFOA). 2017a.

United State Environmental Protection Agency. Basic information on PFAS. 2017b https://www.epa.gov/pfas/basic-information-pfas

United State Environmental Protection Agency. Drinking water health advisory for perfluorooctanoic acid (PFOA). 2016 https://www.hpcbd.com/Personal-Injury/DuPont-C8/PFOA-Health-Advisory-Final.pdf

Velazquez ALB; Deng Y. Reducing Competition of Pepsin in Aflatoxin Adsorption by Modifying a Smectite with Organic Nutrients. Toxins. 2020, 12(1), 28.

Vierke L; Berger U; Cousins IT Estimation of the acid dissociation constant of perfluoroalkyl carboxylic acids through and experimental investigation of their water-to-air transport. Environ. Sci. Technol 2013, 47(19), 11032–11039. [PubMed: 23952814]

Wang M; Hearon SE; Johnson NM; Phillips TD Development of broad-acting clays for the tight adsorption of benzo[a]pyrene and aldicarb. Applied Clay Sciences. 2019, 168, 196–202.

Wang M; Hearon SE; Phillips TD A high capacity bentonite clay for the sorption of aflatoxins. Food Additives & Contaminants: Part A. 2020, 37(2), 332–341.

Wang M; Hearon SE; Phillips TD Development of enterosorbents that can be added to food and water to reduce toxin exposures during disasters. J. Environ. Sci. Health B. 2019c, 54(6), 514–524. [PubMed: 31014207]

Wang M; Maki CR; Deng Y; Tian Y; Phillips TD Development of high capacity enterosorbents for aflatoxin B1 and other hazardous chemicals. Chem. Res. Toxicol 2017, 3099, 1694–1701.

Wang M; Orr AA; He S; Dalaijamts C Chiu WA; Tamamis P Phillips TD. Montmorillonites can tightly bind glyphosate and paraquat reducing toxin exposures and toxicity. ACS Omega. 2019a, 4(18), 17702–17713. [PubMed: 31681876]

Wang M; Phillips TD Potential applications of clay-based therapy for the reduction of pesticide exposures in humans and animals. Appl. Sci 2019, 9(24), 5325. [PubMed: 32944385]

Wang M; Safe S; Hearon SE; Phillips TD Strong adsorption of polychlorinated biphenyls by processed montmorillonite clays: potential applications as toxin enterosorbents during disasters and floods. Environ. Pollut 2019b, 255(1), 113210. [PubMed: 31542671]

Wang M; Bera G; Mitra K; Wade TL; Knap AH; Phillips TD Tight sorption of arsenic, cadmium, mercury, and lead by edible activated carbon and acid-processed montmorillonite clay. Environ. Sci. Pollut. Res 2020. doi: 10.1007/s11356-020-10973-z

Yu J; Hu J Adsorption of perfluorinated compounds onto activated carbon and activated sludge. J. Environ. Eng 2011, 137(10), 945–951.

Zhang DQ; Zhang WL; Liang YN Adsorption of perfluoroalkyl and polyfluoroalkyl substances (PFASs) from aqueous solution - A review. Sci.Total Environ 2019, 694, 133606. [PubMed: 31401505]

Zhao L; Bian J; Zhang Y; Zhu L; Liu Z Comparison of the sorption behaviors and mechanisms of perfluorosulfonates and perfluorocarboxylic acids on three kinds of clay minerals. Chemosphere. 2014, 114, 51–58. [PubMed: 25113183]

Zhi Y; Liu J Surface modification of activated carbon for enhanced adsorption of perfluoroalkyl acids from aqueous solutions. Chemosphere. 2016, 144, 1224–1232. [PubMed: 26469934]

Zhou Q; Deng S; Yu Q; Zhang Q; Yu G; Huang J; He H Sorption of perfluorooctane sulfonate on organo-montmorillonites. Chemosphere. 2010, 78, 688–694. [PubMed: 20042218]

HIGHLIGHTS

- Nutrient-amended montmorillonite clays were shown to strongly bind PFAS
- PFOA, PFOS, and mixtures of PFAS were tightly adsorbed within interlayers of clays
- Hydrophobic/electrostatic interactions and hydrogen bonds were involved in sorption
- Computer modeling and MD simulations validated our experimental results
- Low doses of sorbents protected a *PFAS-sensitive organism* from toxicity of PFAS

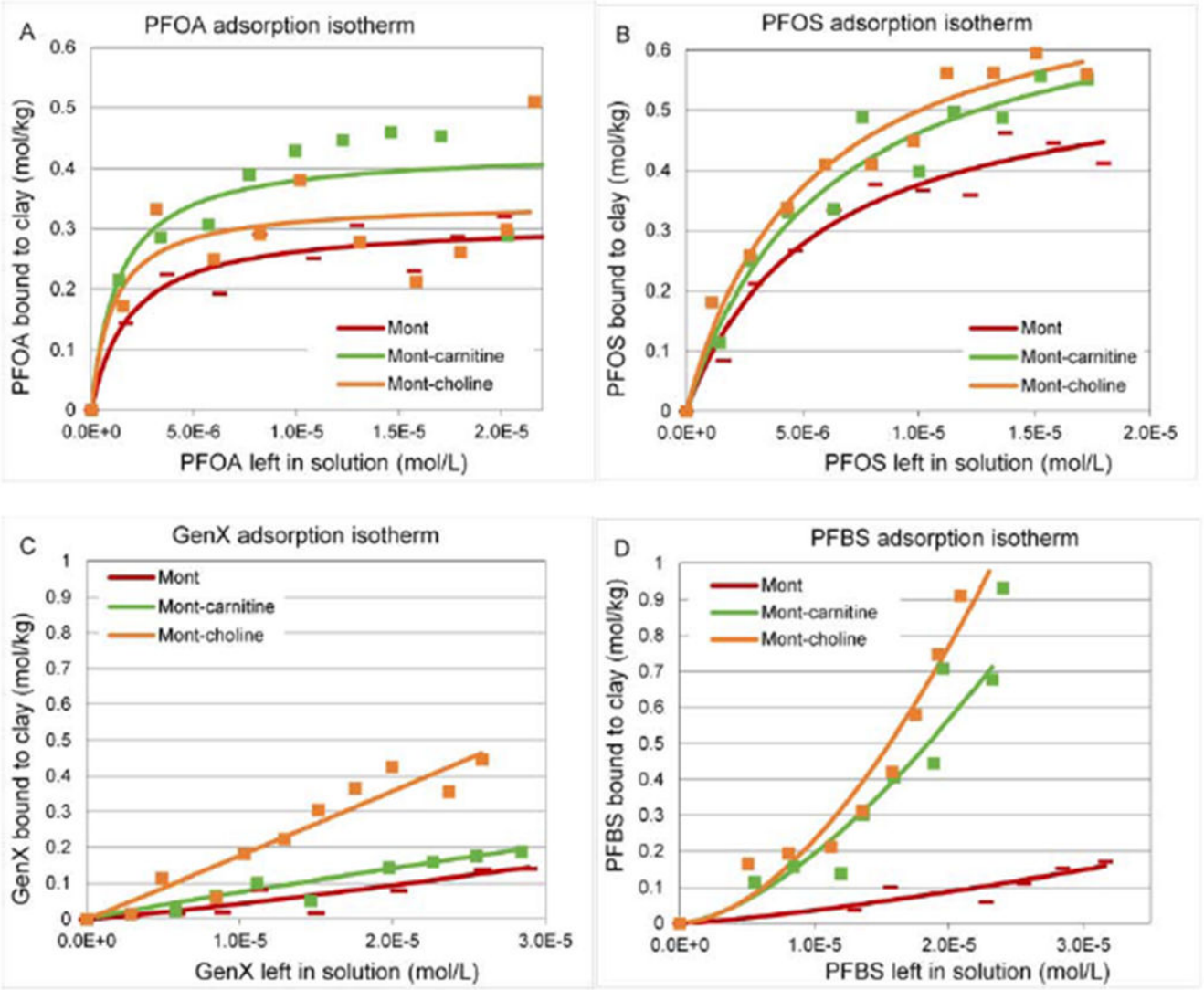

Figure 1.

Adsorption isotherms of PFOA (A), PFOS (B), GenX (C), and PFBS (D) onto parent and amended montmorillonite clays at 37°C, plotted with Langmuir (A and B) and Freundlich (C and D) models. Data represent the mean adsorption (mol/kg) at each concentration, run in triplicate.

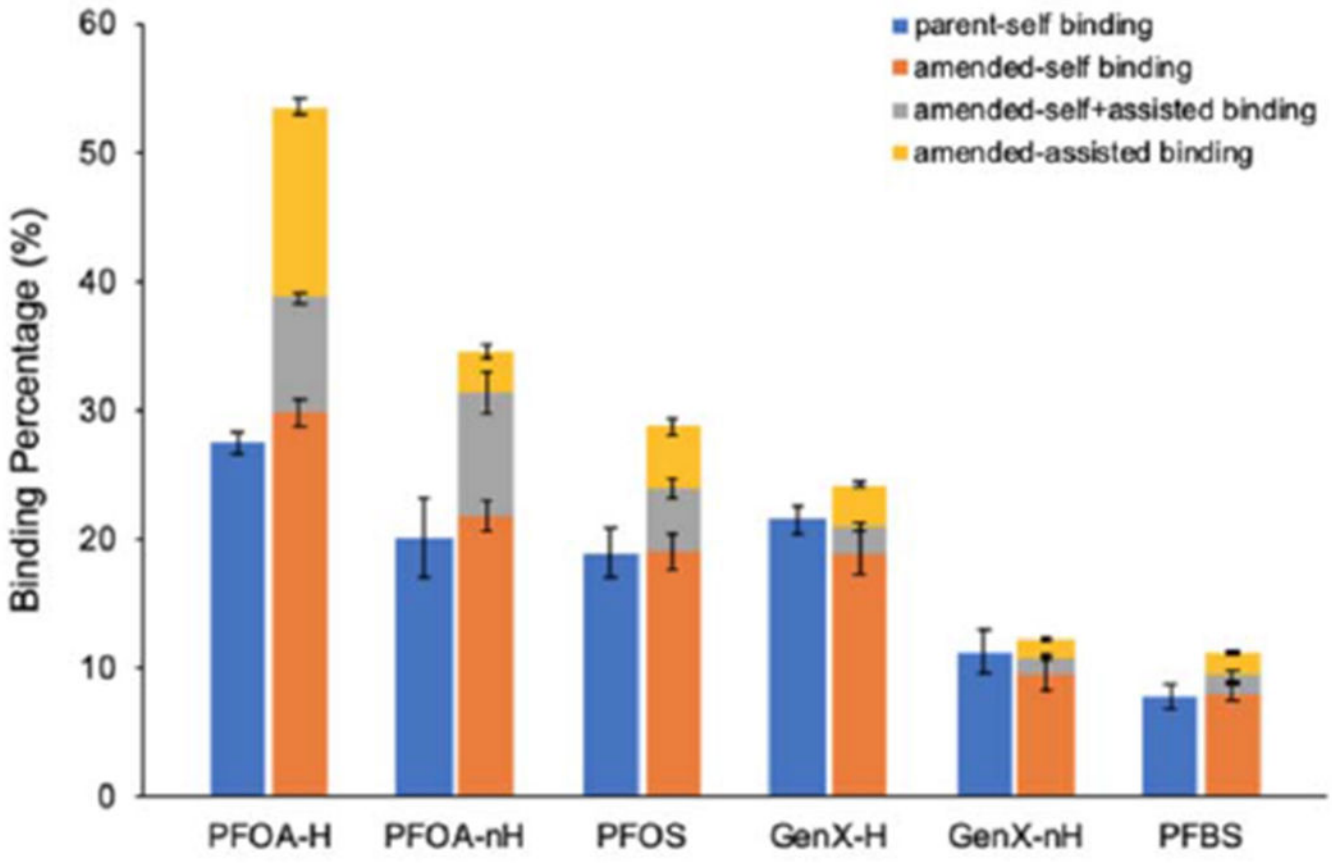

Figure 2.

Binding percentages of the parent clay (blue bars) and mont-carnitine (orange, grey, and yellow bars) for protonated PFOA-H, deprotonated PFOA-nH, PFOS, protonated GenX-H, deprotonated GenX-nH, and PFBS. Orange bars correspond to self-binding instances in which PFAS is bound directly to the clay (without contacting amending carnitines), grey bars correspond to assisted-binding instances in which PFAS is simultaneously bound to both clay and carnitine, and yellow bars correspond to assisted-binding instances in which PFAS is bound to carnitine (without contacting the clay interlayer). Error bars correspond to the standard error across the quintet MD simulations.

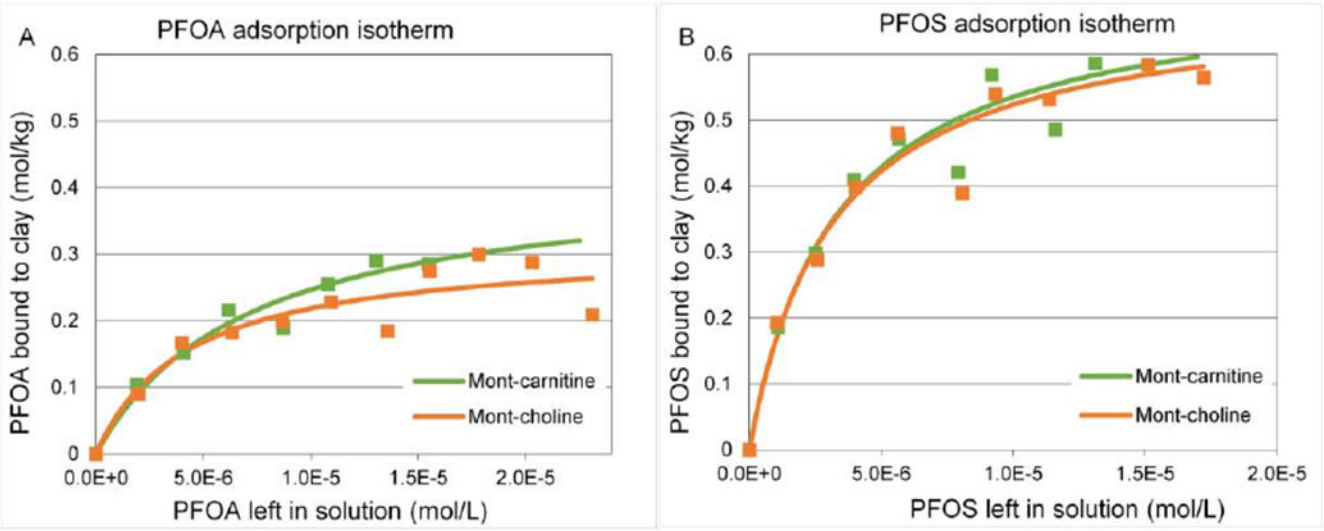

Figure 3.

Adsorption isotherms of co-exposure to PFOA (A) and PFOS (B) onto montmorillonite clays at 37°C, plotted with a Langmuir model. Data represent the mean adsorption (mol/kg) at each concentration, run in triplicate.

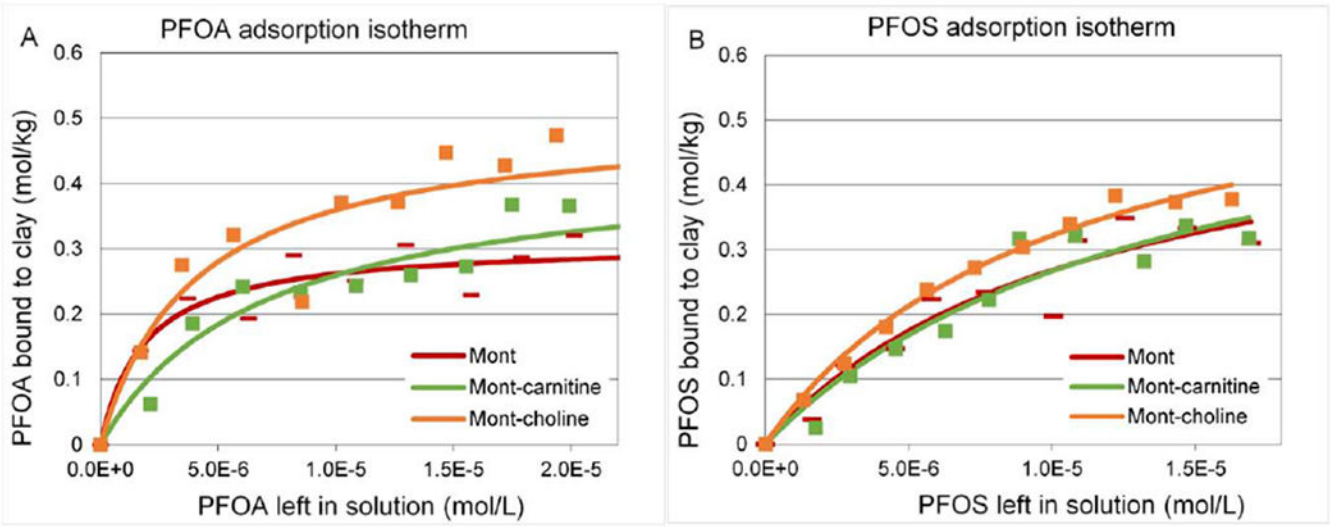

Figure 4.

Adsorption isotherms of PFOA (A) and PFOS (B) onto parent and amended montmorillonite clays at 24°C, plotted with a Langmuir model. Data represent the mean adsorption (mol/kg) at each concentration, run in triplicate.

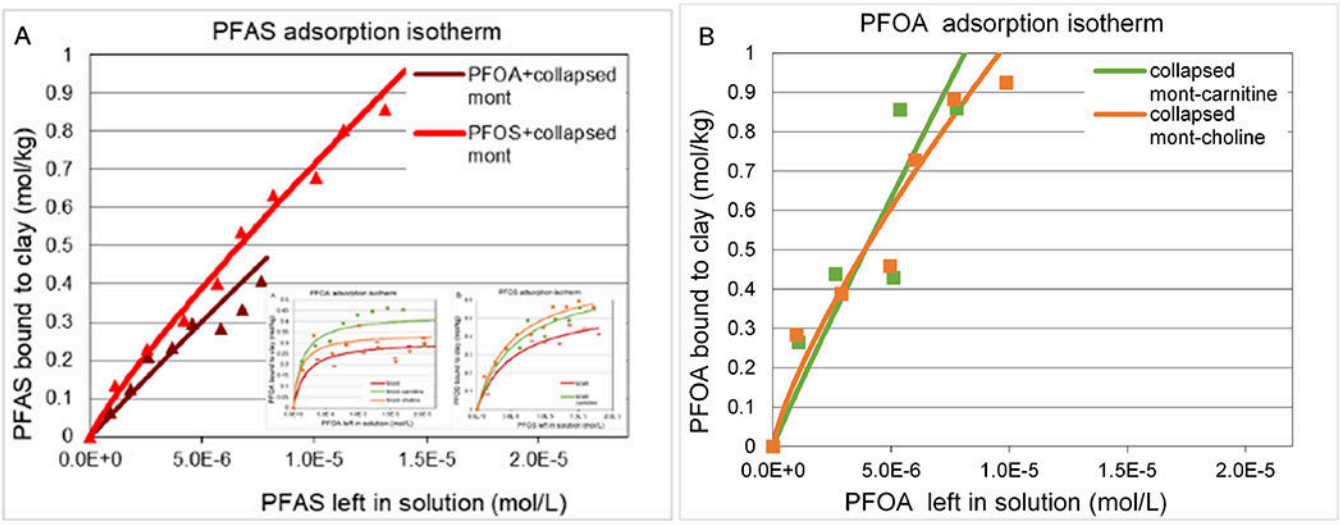

Figure 5.

Adsorption isotherms of PFOA and PFOS onto collapsed montmorillonite clay (A), and PFOA onto collapsed amended montmorillonite clays (B), plotted with a Freundlich model. Data represent the mean adsorption (mol/kg) at each concentration, run in triplicate.

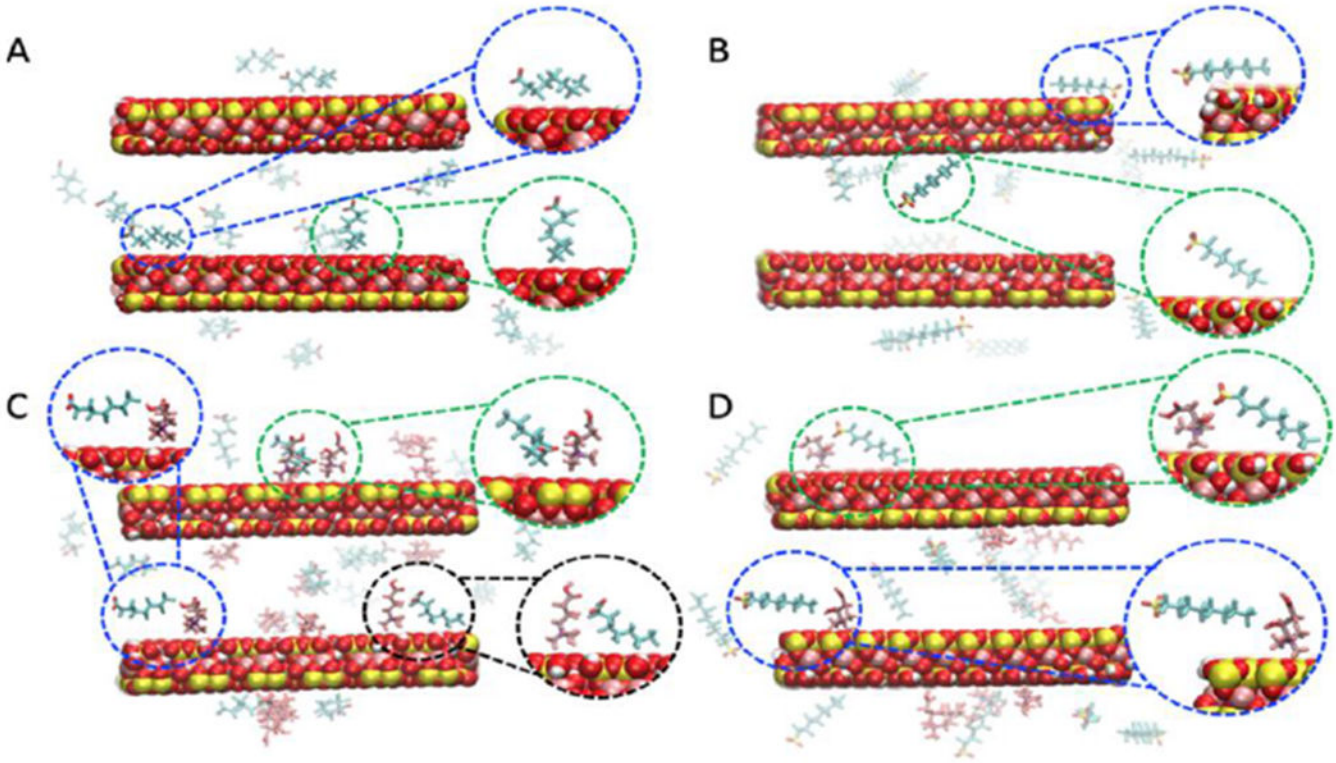

Figure 6.

Molecular graphics of the simulation snapshots containing representative and prominent binding modes for (A) deprotonated PFOA-nH and (B) PFOS binding to the parent clay, and (C) deprotonated PFOA-nH and (D) PFOS binding to mont-carnitine. Zoomed in images of the prominent binding modes are encircled by dotted lines and reoriented to facilitate the comparison of different binding modes. Water molecules are omitted for clarity.

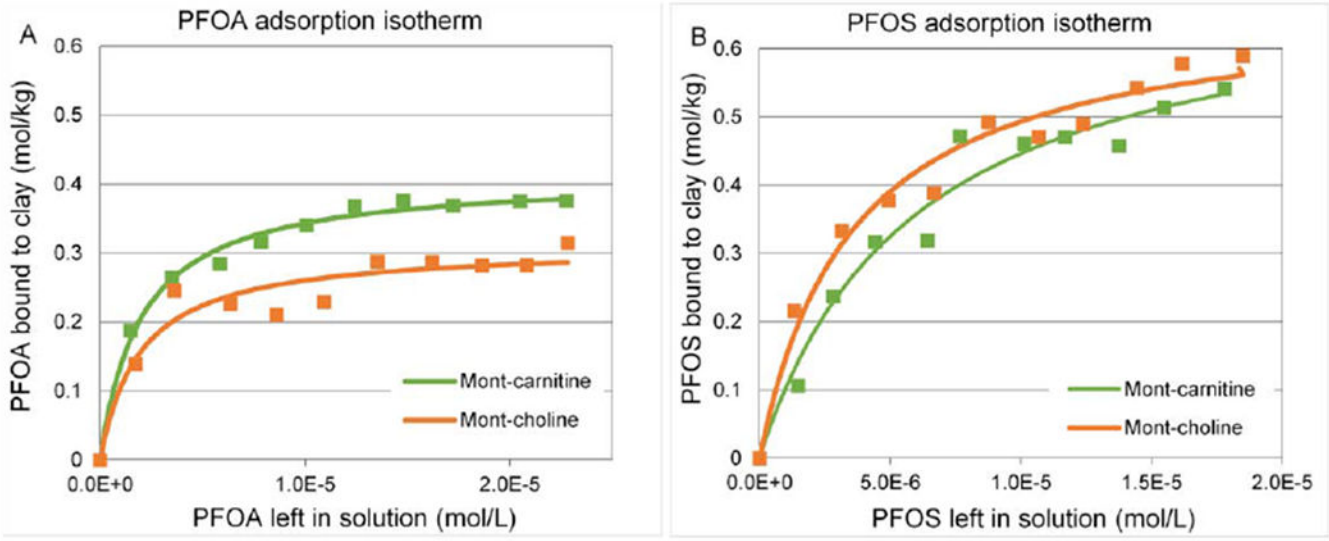

Figure 7.

Desorption isotherms of PFOA (A) and PFOS (B) onto amended montmorillonite clays at 37°C, plotted with a Langmuir model. Data represent the mean adsorption (mol/kg) at each concentration, run in triplicate.

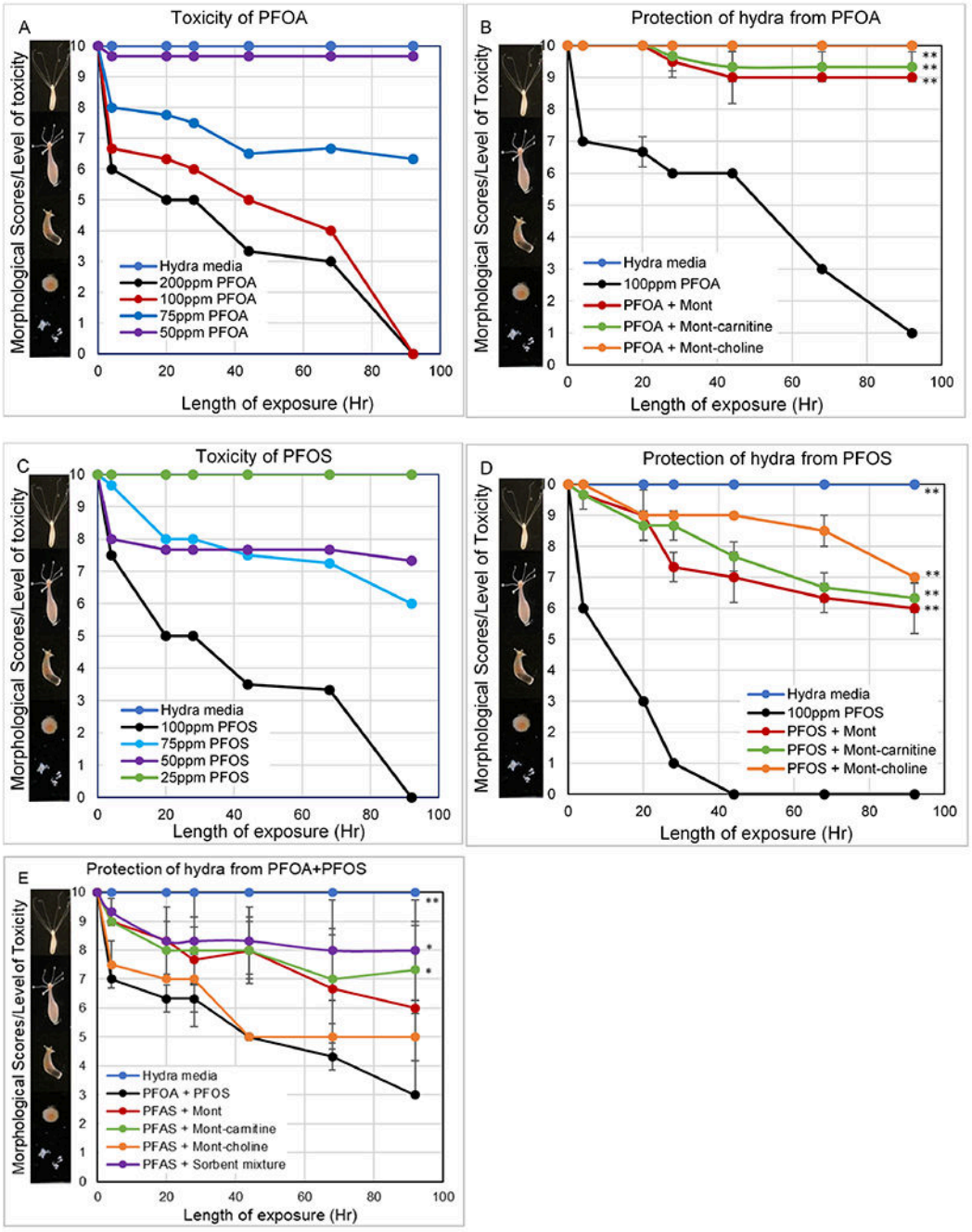

Figure 8.

Hydra toxicity from PFOA (A), PFOS (C) and a mixture (E), and protection by sorbents at an inclusion rate of 0.02% (B, D, E). Hydra medium and toxicant controls are included for comparison. Data represent the mean morphological score at each time point, run in triplicate (* $p \leq 0.05$, ** $p \leq 0.01$).

Table 1.

Important parameters and correlation coefficients derived from adsorption isotherms

Chemical	Montmorillonite			Mont-carnitine			Mont-choline		
				Langmuir					
	Q_{max}	K_d	r^2	Q_{max}	K_d	r^2	Q_{max}	K_d	r^2
PFOA 37°C	0.31	5.37E5	0.89	0.43	7.48E5	0.82	0.34	9.47E5	0.8
PFOA 24°C	0.29	2.04E5	0.95	0.44	1.45E5	0.91	0.5	2.53E5	0.86
PFOA co-exposure 37°C		N/A		0.42	1.42E5	0.96	0.31	2.33E5	0.87
PFOS 37°C	0.58	1.81E5	0.96	0.73	1.69E5	0.96	0.75	1.95E5	0.97
PFOS 24°C	0.58	8.7E4	0.91	0.61	7.16E4	0.92	0.65	9.67E5	0.99
PFOS co-exposure 37°C		N/A		0.71	3.02E5	0.96	0.69	3.19E5	0.95
				Freundlich					
	1/n	K_f	r^2	1/n	K_f	r^2	1/n	K_f	r^2
GenX 37°C	1.14	2.12E4	0.92	0.9	2.52E3	0.98	1.02	2.23E4	0.91
PFBS 37°C	1.28	9.04E4	0.83	1.55	1.1E7	0.91	1.73	1.03E8	0.97

Q_{max}, binding capacity; K_d, binding affinity; r^2, correlation coefficient; 1/n, degree of heterogenicity; K_f, Freundlich distribution constant

Table 2.

Important parameters and correlation coefficients derived from desorption isotherms

Chemical	Mont-carnitine				Mont-choline			
	q_{max}	K_d	r^2	Desorption%	q_{max}	K_d	r^2	Desorption%
PFOA	0.411	5.0E5	0.99	4.64%	0.311	5.17E5	0.92	9.59%
PFOS	0.712	1.68E5	0.97	3.13%	0.669	1.95E5	0.97	11.2%

q_{max}, binding capacity of sorbent following desorption; K_d, binding affinity; r^2, correlation coefficient